J. Phys. D: Appl. Phys. **41** (2008) 025303 (12pp) doi:10.1088/0022-3727/41/2/025303

Noise and switching phenomena in thick-film resistors

A Kolek[1], A W Stadler[1], Z Zawiślak[1], K Mleczko[1] and A Dziedzic[2]

[1] Department of Electronics Fundamentals, Rzeszów University of Technology, W. Pola 2, 35-959 Rzeszów, Poland
[2] Faculty of Microsystem Electronics and Photonics, Wrocław University of Technology, Wybrzeże Wyspiańskiego 27, 50-370 Wrocław, Poland

E-mail: akoleknd@prz.edu.pl

Received 3 September 2007, in final form 12 November 2007
Published 21 December 2007
Online at stacks.iop.org/JPhysD/41/025303

Abstract
Low frequency noise spectroscopy is employed to examine fluctuating phenomena that take place in the material of resistive films and in the film/termination interface of a thick-film resistor. It has been found that the excess low frequency noise apart from the $1/f$ component contains contributions from thermally activated noise sources with energies in the range 0.015–0.6 eV. These sources are nonuniformly distributed over the whole resistor volume, most probably in the glassy matrix or conductive grain boundaries. All noise sources are subjected to the switching phenomenon which abruptly changes the densities of local currents that describe the coupling of the resistance to noise processes produced in the fluctuators. Redistribution of currents results in switching between different sets of active noise sources that build up the noise spectrum. Extensive experimental studies that consider the influence of various parameters of fabrication process, sample geometry, substrate and operation exposures suggest that the most likely origin of the switching phenomenon is the relaxation of mechanical stress which in thick-film resistors appears due to the mismatch of the thermal expansion coefficients of the materials contained in resistive films, conductive terminations and the substrate.

(Some figures in this article are in colour only in the electronic version)

1. Introduction

Thick-film resistors (TFRs) although known as relatively low-noise components of electronic circuits still suffer from low frequency noise which becomes dominant below a few kilohertz. Hence their use in precision electronics and newly developed sensor applications is considerably limited. This fact stimulates research directed on the recognition of the conducting mechanism, which is still unknown, establishing criteria of low-noise devices [1] and relationships between noise and important device utilities such as quality, reliability [2] and long-term stability [3]. Although many papers address the issues raised above, little progress in the field has been done and there is still much work to do. So far noise has been tested against, e.g. biasing voltage, temperature, device volume, material composition, loading factor and granularity, termination metallurgy, firing temperature, substrate, trimming method and trimming cut geometry. In spite of extensive experimental studies, noise mechanism in thick resistive films is still unknown and the main reason for this is that little is known about the conduction mechanism in general. To some extent the lack of a theoretical model stimulates noise studies which are expected to gain supplementary information that may help to find out the fundamental process of electrical transport. Our paper adds several contributions to this aspect. We have found that low frequency noise at least in part (if not completely) is generated by thermally activated noise sources (TANSs) [4] which are nonuniformly scattered within the material of resistive films, including the film/termination interface. Physically, such noise sources could be two-level systems existing in the glassy matrix of TFR [5], which couple to resistance via the modulation of barrier heights for tunnelling transitions in conduction paths.

Another phenomenon, unreported to date, are microswitchings which are probably connected with mechanical stress relief. Observation of these switchings was possible due to the use of low frequency noise spectroscopy [6] which occurred to be an extremely sensitive tool for detecting

 © 2008 IOP Publishing Ltd Printed in the UK

this kind of phenomena. The relation between microswitchings and stress relief is of large practical importance as the latter affects the long-term stability of TFR [7]. This aspect combines with another issue addressed in the paper which is the use of information stored in the noise signal to quantify the utility performance of various materials used in thick-film technology and to describe pastes' compatibility and technological conditions for optimal manufacturing. During TFR firing many interactions take place between conductive filler and glass, conductive filler and modifiers, glass and modifiers as well as between components of resistive film and substrate or components of resistive film and terminations [8]. Most of these interactions are far from being well understood but lead to important observable effects. In the exemplary case of the interactions between resistive film and conductive termination either direct or inverse 'size' effects are usually observed. For example, for RuO_2-based films, Ag-containing terminations and Al-containing glass or substrate the increase in resistivity near the terminations extends up to hundreds of millimetres in depth of the resistive layer [9]. However, the change in local resistivity is barely the first order effect reflecting averaged chemical, mechanical, thermal and electro-physical reactions between materials of the films that built up the interface. Higher order effects such as contact homogeneity, density of time varying defects, crack corrosion and others can be inspected using low frequency noise as a diagnostic tool. It is well known that contacts (if bad) can produce extraordinary noise, which can be even larger than the noise produced inside a device. In the paper it is proposed to get some insights into the phenomena that take place in resistive films, film/substrate and film/termination interfaces by the use of low frequency noise spectroscopy applied to various parts of TFR made of various resistive and conductive pastes and formed on various substrates. Measurements reveal that for some resistive/conductive systems the population and/or intensity of TANSs increase in the film/termination interface. Moreover, experiments show that in many cases switching phenomena in the interface are more frequent than in the bulk of the resistor. This observation adds new criteria to the definition of pastes' compatibility.

Although conclusions derived in the paper are mainly of practical importance, our experimental data are quite new in general, since only few experimental studies address the problem of temperature dependence of low frequency noise in TFRs [10–12]. In [10] measurements similar to ours confirmed the existence of TANS with an activation energy of $E_a \cong 1.52\,\text{eV}$. Our finding is that TANSs have energies in the range 0.015–0.6 eV and are a property common for all sorts of TFRs.

The paper is organized as follows. In section 2 the basic experimental tool—method of low frequency noise spectroscopy, is briefly described. Further experimental details are described in sections 3 and 4. In section 5 arguments for the existence of TANSs in TFRs are supplied. In subsequent subsections their features are discussed in detail. Switching phenomena, their features and theoretical models are considered in section 6. Section 7 completes experimental characterization of noise and switching phenomena and summarizes the results.

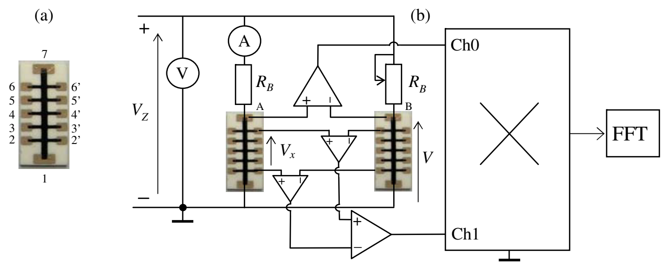

Figure 1. (a) Shape of the samples and contacts enumeration. (b) Setup for noise measurements.

2. Low frequency noise spectroscopy

Noise spectroscopy uses the function of power spectral density $S_V(f)$ of the noise signal $\delta V(t)$, evaluated in a wide frequency range at several (many) temperatures. As the $1/f$ noise dominates at low frequencies the product fS_V gives an appropriate scale to examine features in the noise spectra. Evolution of these features as a function of temperature T is the key point of the method. For TANSs the position f_{max} of the local maximum in $fS_V(f)$ on the frequency axis moves linearly with the reciprocal temperature [4, 6, 10]. Appropriate activation energies can be calculated from Arrhenius plots:

$$\frac{\partial \lg f_{max}}{\partial 1/T} = -\frac{E_a}{k \ln 10}. \quad (1)$$

If there are no features in the noise spectrum one can still consider noise as resulting from the presence of TANSs by a careful inspection of the noise spectral exponent $\gamma \equiv \partial \ln S_V(f)/\partial \ln f$. The theory of Dutta, Dimon and Horn (DDH) [4] relates γ to the temperature dependence of the noise through the relation

$$\gamma = 1 - \frac{1}{\ln \pi \tau_0 f}\left(\frac{\partial \ln S_V}{\partial \ln T} - 1\right), \quad (2)$$

where τ_0 is the attempt time of making transitions in noise sources. If this relation holds, thermally activated transitions are expected to occur between the states of approximately equal energy [4].

3. Samples

In the experiments the noise signal is to be taken from various parts of a resistor, so the samples were prepared as multiterminal specimens with several side legs equally spaced along the resistor length (see figure 1(a)). The distance between successive legs as well as between first/last leg and adjacent current termination measured along the main film was 2.5 mm. The total length of the sample's resistive film was $L = 15$ mm.

Resistive films were made of the following.

- Lab-made pastes with ruthenium dioxide and lead-borosilicate glass (10% B_2O_3, 15% SiO_2, 65% PbO) as basic components. The fraction υ of RuO_2 was either 10% or 12% by volume.

- Commercially available RuO_2-based pastes DP2021, DP2031 and DP2041 from DuPont and R343 and R344 from ITME (Institute of Electronic Materials Technology, Warsaw, Poland). Paste R344 of sheet resistance 10 kΩ/□, contains ∼36% of bismuth ruthenate as conductive material and the mixture of two glasses, PbO–SiO_2–Al_2O_3 and B_2O_3–SiO_2–CaO–BaO–NiO–SnO, as hosting insulator. Paste R343 of sheet resistance 1 kΩ/□ is a fifty–fifty composition of $Bi_2Ru_2O_7$ and PbO–SiO_2–Al_2O_3 glass with a small ingredient of $ZrSiO_4$ [13].

It is important to realize that resistive pastes are the mixture of conducting and insulating components so the resistor in the final form is a metal–insulator composite. Experiments however, show, that atoms/molecules of conducting component diffuse into the glass: hence electrical properties of the insulator are considerably modified [14].

Current pads and voltage side contacts to the resistors were made of pastes containing Au, Pt, Pd and Ag as basic ingredients. There were used commercially available pastes from:

- ITME, products: P303 (Au) and P304 (Au and Pt),
- Metech, products: 3505 (PdAg), 1130C (PtAg), and 3612 (Au),
- DuPont, products: DP6146 (PdAg) compatible with 951 green tape (LTCC technology) and DP6453—photoprintable silver-based fine-line Fodel ink and
- Electro-Science Laboratories, product ESL8880H (Au).

Resistors for measurements were manufactured:

- in a conventional 'high temperature' process on alumina substrates; samples were screen printed through a 200 mesh screen and after firing at the peak temperature, $T_p = 800\,^\circ$C or $850\,^\circ$C or $900\,^\circ$C, for 10 min gained the average thickness of 10–20 μm,
- as LTCC resistors on DuPont green tape DP 951 as surface devices; substrate (ceramic) and resistors were fired together (co-firing process) or separately (post-fired process),
- as 150 μm wide microresistors made of DP2031 resistive ink screen printed on alumina substrates and fired at $850\,^\circ$C with contacts made in the Fodel process [15],

Resistors were fabricated in series of 8 specimens. From each series a pair of samples with nearly matching resistance between contacts 1–7, $R \equiv R_{1-7}$ (see figure 1(*a*)), at room temperature was selected for noise measurements. For each pair the measurements were made on as-prepared devices and also after annealing at $120\,^\circ$C for 1000 h. Such ageing was used in many experimental studies, e.g. in [16, 17] in order to simulate the lifetime of 20 years at normal operation (at $70\,^\circ$C).

The set of samples was designed and prepared with the intent to (i) examine the influence of various parameters of fabrication process, sample geometry, substrate and operation exposures on noise phenomena in TFRs, (ii) establish the role of resistive layer and film/termination interface in noise generation and (iii) formulate new criteria of conductive/resistive pastes' compatibility.

4. Measurement setup

The setup for noise measurements is shown in figure 1(*b*). It has the advantage of crosscorrelation technique and bridge configuration. For the arrangement of input signals as in the figure, the noise generated in the portion of the main film that extends between contacts 6 and 2 (sectors 2–6) is calculated as the cross power spectral density of voltage V measured in channel Ch0 and voltage $V_x = V_{2-6}$ measured in channel Ch1. Such a cross power spectrum scales linearly with the inter-leg distance [18], so that the spectra measured for sectors between successive neighbouring legs add up to give the spectrum for the whole resistor. The latter is measured directly in Ch0 as the ordinary power spectral density of voltage V. It is important that both quantities S_V and S_{VVx} are measured simultaneously. Spectra of the background noise are measured in the same way, setting bias V_Z to zero. At high frequencies $S_{V=0}$ is dominated by thermal (Johnson) noise of the resistors, $S_{V=0} = 4kTR$. At low frequencies it takes the value of the preamplifier noise. The difference $S_{V_{\rm ex}} \equiv S_V - S_{V=0}$ ($S_{V_{\rm ex}} \equiv S_{VVx} - S_{VVx=0}$ for sector quantities) defines the spectrum of excess noise. Examples of such a spectrum in the form of $fS_{V_{\rm ex}}$ versus f plots are shown in figure 2. All amplifiers in figure 1(*b*) were ac-coupled to the samples with the cutoff frequency slightly less then 1 Hz, so the spectra in figure 2 and many others shown in the following sections refer to the fluctuating part of the measured quantities above this frequency.

In the setup of figure 1(*b*) load resistances $R_{\rm B}$ fulfil the condition $R_B \gg R$. During measurements they remain in room temperature, while the samples are cooled in a liquid nitrogen cryostat. Volt- and ammeters enable the measurement of sample resistance R simultaneously with acquisition of noise spectra. For most samples R decreases with increasing temperature. Only for low-resistive samples $R(T)$ runs through a wide minimum. For any of the samples the absolute value of the temperature coefficient of resistance $\beta \equiv {\rm d}\ln R/{\rm d}T$ never exceeds 1000 ppm K^{-1}. With this value it is possible to estimate the variance of resistance fluctuations resulting from temperature fluctuations [19]:

$$\langle \delta R^2 \rangle = R^2\beta^2 kT^2/C_V < 10^{-7}\Omega^2, \qquad (3)$$

where C_V is the heat capacity of the sample. When calculating the upper limit of $\langle \delta R^2 \rangle$ we have used the maximum value of samples' resistance $\sim 10^5\ \Omega$ and assume that heat capacity is determined by the glassy constituent of the films. Then $C_V = c_v\rho\Omega$ where the sample volume $\Omega \sim 10^{-10}$ m^3, specific heat of the glass $c_v \sim 0.2$–0.9 J g^{-1} K^{-1} [20] and its density $\rho \sim 4$ g cm^{-3}. The value on the rhs of (3) is several orders of magnitude lower than any of the mean square fluctuations measured in the experiments. The latter, though measured in the limited frequency band, were always greater than $10^{-5}\Omega^2$ (see figures 3, 6, 8–13). Thus, the contribution from temperature fluctuations to the measured noise is negligible.

5. Thermally activated noise sources

Noise spectra $S_V(f)$ were measured as a function of temperature. In figure 2(*b*) they are presented as $fS_V(f)$ in

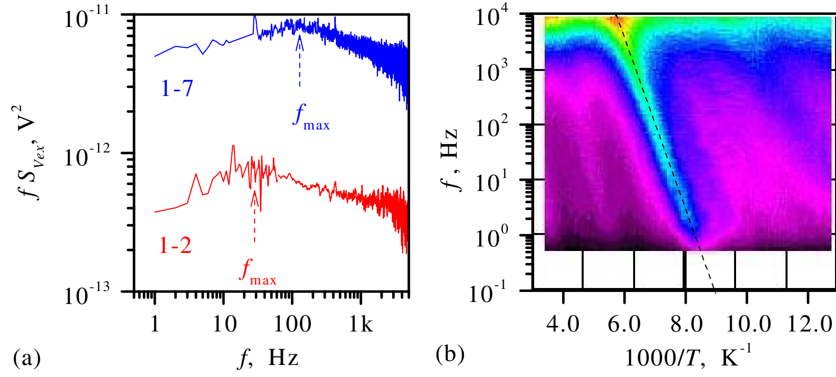

Figure 2. Product of frequency and noise power spectral density measured (*a*) for various parts of the v10RuO$_2$/P303Au resistor at room temperature and (*b*) for the whole resistor as a function of temperature. In both cases measurements were done for the bias $I \cong V_Z/R_B = 0.39$ mA. In (*b*) $f S_V(f)$ is mapped according to black (dark) (lowest value) and red (lighter) (highest value) scheme versus frequency f and reciprocal temperature. (Colour online.)

the form of a two-dimensional (2D) map versus frequency and $1000/T$. The product $f S_V(f)$ increases at high frequencies due to thermal noise which above a few kilohertz overlaps the $1/f$ noise and makes $f S_V(f) \cong 4kTRf$ to linearly increase with f. Streaks on the map show migration of the local maxima with the temperature. The dashed line drawn along the main streak confirms that $f_{\max}$ depends on $1/T$ linearly and so the thermally activated random process is responsible for showing this feature in the noise spectrum. The corresponding activation energy of $E_a = 0.305$ eV is calculated from the slope of this line by virtue of equation (1).

Experiments performed on various samples in the temperature range 77–300 K show the following.

- TANSs produce excess noise. They were never observed without bias.
- TANSs couple to film resistivity (produce resistance noise).
- TANSs are small objects localized in a glassy matrix or conductive grain boundaries.
- Each sample has several TANSs with different activation energies (streaks with different slopes have been observed). Even the samples made from the same resistive/conductive pastes have different sets of TANSs.
- TANSs are nonuniformly distributed within the resistive film (different sectors occurred to have different streaks).
- On average the number of TANSs and magnitude of the signal they produce decrease with decreasing sheet resistivity. Samples of low-resistive R343 series have at most two TANSs (in the temperature and frequency ranges of interest). An exception are LTCC resistors for which TANSs are extremely rare even for high resistive samples.
- Decreasing firing temperature makes TANS less intensive and frequent.
- Annealing does not remove TANSs.
- TANSs are a common property (streaks have been found for almost all studied samples).
- Population and/or intensity of TANSs increase in the film-termination interface.
- TANSs are highly influenced by the switching process triggered by microstructure changes.

In the following some of these features are discussed in more detail.

5.1. Resistance fluctuations

The statement that TANSs produce resistance fluctuations needs more arguments. Coupling a random process to resistivity results in resistance fluctuations. For the measurement setup of figure 1(*b*) with nearly constant current bias $I \cong V_Z/R_B$, resistance fluctuations should result in voltage fluctuations that increase linearly with I (and V), $\delta V = I\delta R \sim V\delta R$. The experiment confirms this behaviour. At a fixed temperature noise was measured for several biasing voltages including $V = V_Z = 0$. The magnitude of excess noise (noise power) was then calculated as the mean square voltage

$$\langle \delta V_{\mathrm{ex}}^2 \rangle \equiv \int_{f_L}^{f_H} \mathrm{d}f \, S_{V_{\mathrm{ex}}}(f),$$

integrating the power spectral density $S_{V_{\mathrm{ex}}}(f)$ over the band $\Delta f = f_H - f_L$ which contains the feature in the noise spectrum. In the case of the spectrum for sector 1–2 with $f_{\max} \cong 30$ Hz (see figure 2(*a*)) this band was fixed between 1 and 200 Hz. $\langle \delta V_{\mathrm{ex}}^2 \rangle$ occurred to scale linearly with V^2, exactly like the resistance origin that the noise predicts. Moreover, the remaining part of the spectrum, where $1/f$ noise dominates ($f S_{V_{\mathrm{ex}}}(f)$ is flat), also scaled linearly with V^2 and so this noise is also of the resistance type which is a well-known fact [21].

Power spectral density of resistance fluctuations can be calculated as $S_R(f) = S_{V_{\mathrm{ex}}}(f)/I^2$, where I is the current flowing through the sample and is directly measured in the measurement setup of figure 1(*b*). Its value does not influence the result but too large current densities may cause self-heating of the samples. This is likely to happen at low temperatures. Fortunately, at 77 K our resistors are fairly sensitive to temperature changes and so self-heating can be controlled by the measurement of sample resistance while increasing the current. All measurements were done for current densities low enough to prevent self-heating and keep the samples in the linear regime where the value of the resistance noise does not depend on the biasing current. The

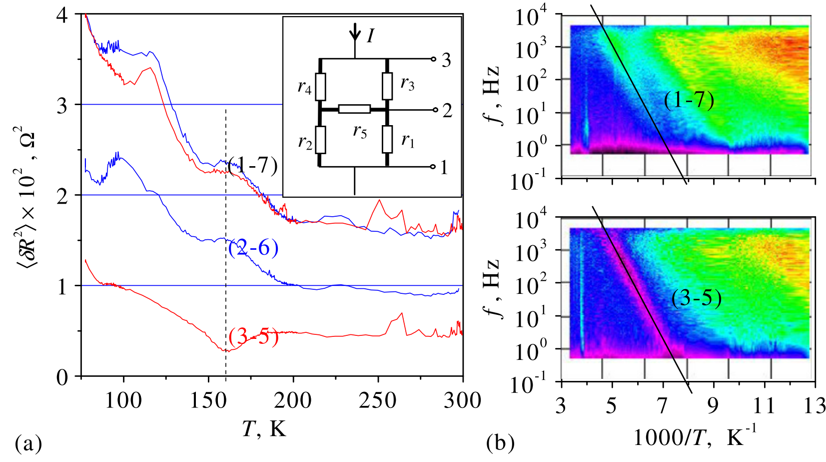

Figure 3. (*a*) Noise power (resistance fluctuations) versus temperature measured between different pairs of contacts of the R344/1130CPtAg resistor. Inset: lumped model of a resistor. (*b*) Map of the product $f S_V(f, T)$ recorded simultaneously on terminations 1–7 (upper) and 3–5 (lower). Bias was $I \cong 97\,\mu$A. The line shows TANS of $E_a = 0.29$ eV.

largest current densities were applied to low-resistive samples and never exceeded 50 A cm^{-2}.

5.2. *Glass/grain boundary localization*

Useful information can be inferred from the amplitude dependence of TANS. As already mentioned DDH derived their relation (2) assuming that thermally activated transitions occur between the states of approximately equal energy [4]. Calculations made on several sets of our data confirm that the DDH relation holds (see [22] for details). Thus, although the nature of TANS remains unknown, one may conclude that as states of roughly equal energies are unlikely in a pure bulk crystal in thermal equilibrium, most probably the noise is generated when electron transport takes place through grain boundaries and/or localized energy states in the glass. Interestingly, the existence of fluctuating two-level systems in a glassy matrix of TFR, that may produce noise, was postulated by Skrbek *et al* [5] who found them responsible for resistance relaxation observed in carbon and RuO_2 thick-film low-temperature thermometers.

5.3. *Inhomogeneous distribution*

Inhomogeneous distribution of TANSs was observed for almost all samples being examined. The conclusion was made upon the argument that noise maps measured for different sectors of a resistor were different. Care must be taken, however, when drawing conclusions about the spatial allocation of noise sources. In general the statement that the fluctuators that produce streaks on the map are located inside the sector for which the map has been measured is not true. The simple lumped model of a resistor, shown in figure 3 (inset), gives an appropriate example. In this model each arm of letter 'H' has resistance $r_k = r$ with a small fluctuating term δr_k. When the external current I is supplied in the up–down direction, fluctuations of voltage on a pair of side contacts can be calculated with the use of the Vandamme and van Bokhoven [23] result

$$\delta V_x = \sum_{k=1}^{5} \frac{I_k \tilde{I}_k}{I} \delta r_k, \qquad (4)$$

where $V_x = V_{1-2}$, V_{3-2} or V_{1-3} and I_k and $\tilde{I}_k$ are the currents in arm k ($k = 1, 2, \ldots, 5$) which flow in original and adjoint networks, respectively. The adjoint network is the network in which current I is supplied from respective voltage probes whereas current taps are hanging. In our experiment noise powers of different sectors were measured with the cross correlation technique, i.e. as $\langle \delta V \delta V_x \rangle$ [18]. For $V = V_{1-3}$, $V_x = V_{1-2}$ and uncorrelated local noise sources, $\langle \delta r_k \delta r_{k'} \rangle = 0$ for $k \neq k'$, we get

$$\langle \delta V \delta V_x \rangle = \sum_{k=1}^{5} \frac{I_k^3 \tilde{I}_k}{I^2} \langle \delta r_k^2 \rangle = I^2 \left[\left(\frac{1}{2}\right)^3 \frac{5}{8} \langle \delta r_1^2 \rangle + \left(\frac{1}{2}\right)^3 \frac{3}{8} \langle \delta r_2^2 \rangle + \left(\frac{1}{2}\right)^3 \frac{-1}{8} \langle \delta r_3^2 \rangle + \left(\frac{1}{2}\right)^3 \frac{1}{8} \langle \delta r_4^2 \rangle \right]. \qquad (5)$$

For uniformly distributed noise sources $\langle \delta r_k \delta r_k \rangle = a$ for $k = 1, 2, \ldots, 5$, the last two terms of the sum on the rhs of (5) cancel out and $\langle \delta V \delta V_{1-2} \rangle / I^2 = a/8$. Calculations for $V_x = V_{2-3}$ and $V_x = V_{1-3}$ give $\langle \delta V \delta V_{2-3} \rangle = \langle \delta V \delta V_{1-2} \rangle$ and $\langle \delta V \delta V_{1-3} \rangle = \langle \delta V \delta V_{1-2} \rangle + \langle \delta V \delta V_{2-3} \rangle$, that is, for uniformly distributed noise sources noise power scales linearly with the sample length.

The case of nonuniformly distributed noise sources can be illustrated, e.g. when all but one noise generators have equal powers $\langle \delta r_k \delta r_k \rangle = a$ for $k = 1, 2, 4, 5$, whereas δr_3 contains additional, e.g. thermally activated component, $\langle \delta r_3 \delta r_3 \rangle = a + b$, $b \equiv \langle \delta r_{\mathrm{TANS}} \delta r_{\mathrm{TANS}} \rangle$. Then we get $\langle \delta V \delta V_{1-2} \rangle / I^2 = a/8 - b/64$, $\langle \delta V \delta V_{2-3} \rangle / I^2 = a/8 + 5b/64$ and $\langle \delta V \delta V_{1-3} \rangle / I^2 = a/4 + b/16$. Values for sectors 1–2 and 2–3 still add up to give the value for sector 1–3, $\langle \delta V \delta V_{1-3} \rangle = \langle \delta V \delta V_{1-2} \rangle + \langle \delta V \delta V_{2-3} \rangle$ like in the case of homogeneous distribution of noise sources, but now $\langle \delta V \delta V_{2-3} \rangle \neq \langle \delta V \delta V_{1-2} \rangle$. Moreover, the calculations show that TANS located in sector 2–3 contributes to the noise power

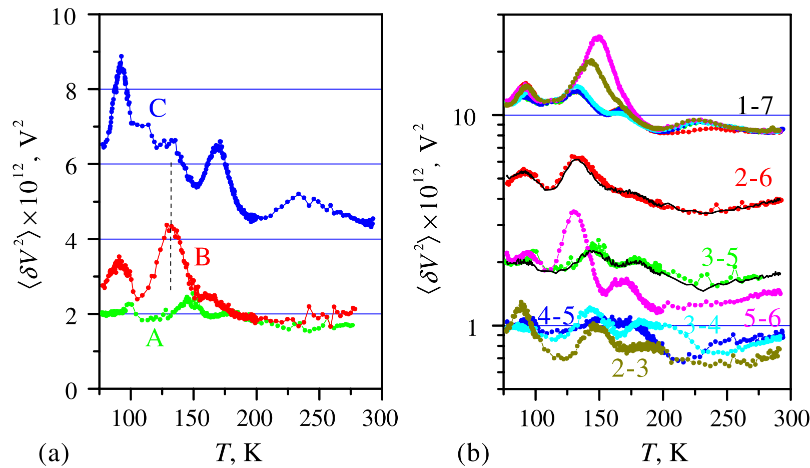

Figure 4. Noise power (voltage fluctuations) in the band 100–1000 Hz versus temperature of the v12RuO$_2$/P304PtAu resistor measured in (*a*) different zones and (*b*) different sectors of the resistor. Lines in (*b*) are the sum of noise powers in sectors 3–4 and 4–5 (lower) and 2–3, 3–4, 4–5 and 5–6 (upper). The most upper plots refer to noise power measured for the whole sample in six temperature cycles. Bias was $I \cong 0.31$ mA.

measured for sector 1–2. It is of negative value but if the TANS were located in arm r_4 instead of r_3 it would produce a positive contribution.

Experimentally, it is not easy to find such a configuration of fluctuators which would confirm the usefulness of the lumped model, being considered above, especially as only those configurations that produce negative contribution can give a recognizable trace. From among several tens of specimens, examined in this study, we were able to find one example. It was the R344/1130CPtAg resistor for which we have found TANS of $E_a = 0.29$ eV, which gave a positive contribution to the noise powers of sectors 2–6 and 1–7 and a negative contribution to the noise power of sector 3–5. Results of this instructive experiment are shown in figure 3. Apart from noise maps taken on terminations 3–5 and 1–7 respective noise powers $\langle \delta R^2 \rangle$ are drawn versus temperature. These powers were calculated in the frequency decade 10–100 Hz integrating (measured) power spectral densities $S_R(f)$. In such a presentation TANSs appear again as local extremes. TANS that produces a moving minimum in the map for sector 3–5 gives a minimum at ~160 K on the $\langle \delta R^2_{3-5} \rangle (T)$ curve. Referring to the lumped model of a resistor, considered above, we may conclude that this TANS is located outside this sector, slightly above contact 5 or slightly below contact 3, on that side of the main film which is close to these contacts. Only this localization is probed by (adjoint) current sufficiently large to give a reasonable negative contribution to noise power measured for sector 3-5. This means that TANSs are objects much smaller than the size of a single-spaced sector.

5.4. Interface noise

The increase in density and/or intensity of TANSs in the film/termination interface was observed for most resistive/conductive paste combinations, e.g. in the experiment on v12RuO$_2$/P304PtAu samples. In figure 4 noise power $\langle \delta V^2 \rangle$ in three zones of the resistors is plotted versus temperature. The zones are of the same size but are located at various distances from resistor terminations. Zone A comprises sectors 3–4 and 4–5, zone B sectors 2–3 and 5–6 and zone C sectors 1–2 and 6–7. The noise magnitude and the number of TANSs increase as the zone is closer to resistor terminations. In zone C, nearest to the terminations, noise is much higher than in other zones and contains four maxima. In contrast, in the most inner zone A the magnitude and number of the maxima are the lowest. An important feature of TANSs located in zone C is that they are either nonstationary or especially sensitive to microstructural changes occurring in TFR during cooling. This property is illustrated in figure 4(*b*), where more data for the v12RuO$_2$/P304PtAu sample are shown. There, the results of six cooling–warming cycles are shown in which noise spectra have been measured in the range 77–300 K for single-spacing sectors 2–3, 3–4, 4–5, 5–6, a two-spacing sector 3–5 and a four-spacing sector 2–6. A simple sum-test shows that noise powers for the single-spacing sectors add up to give noise powers measured for larger sectors, 3–5 and 2–6. As the spectra for different sectors were measured in different experiments this result requires (i) stationary processes at all measured sectors and (ii) minor changes in the resistive film microstructure occurring during successive 77–300 K thermal cycles.

As described in section 4 in each temperature cycle apart from the spectrum for a given sector the spectrum for the whole sample (contacts 1–7) was also measured. If the noise in sectors 1–2 and 6–7 had been stationary, noise power measured on terminations 1–7 in all six experiments would have been identical. This is not the case for figure 4(*b*). Here the maximum at 150 K appears only in two of six '1–7' noise powers and is absent in the other four. This means that TANSs in zone C are either nonstationary (at least on the time scale of the experiment) or thermal cycles introduce substantial microstructural changes into the resistive/conductive films' interface.

6. Nonstationary/microstructural fluctuations

The magnitude of nonstationary (N) or thermal-cycling-developed microstructural (M) fluctuations can be estimated

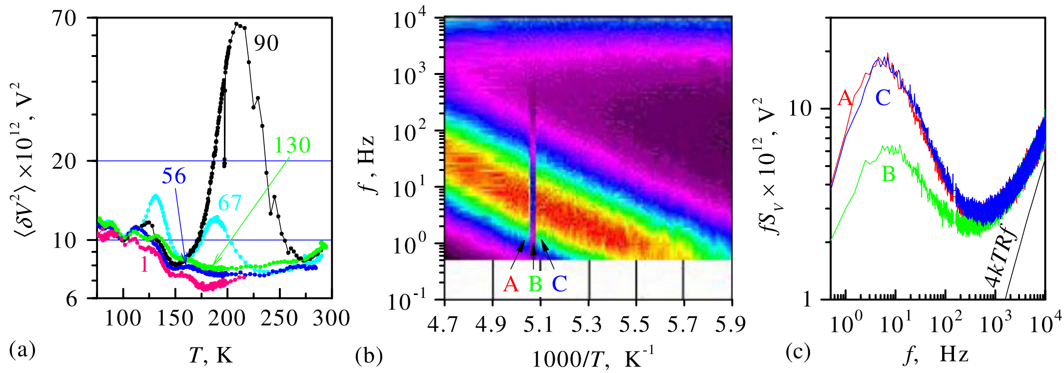

Figure 5. (*a*) Noise power (voltage fluctuations) in the band 10–100 Hz versus temperature measured several times under the bias $I \cong 0.31$ mA for the v12RuO$_2$/P303Au resistor on terminations 1–7. Labels specify the day number on which the measurement was performed. (*b*) Map of the product $f\,S_V(f, T)$ recorded on day 90. (*c*) Noise spectra measured at temperatures marked as A, B, C in (*b*).

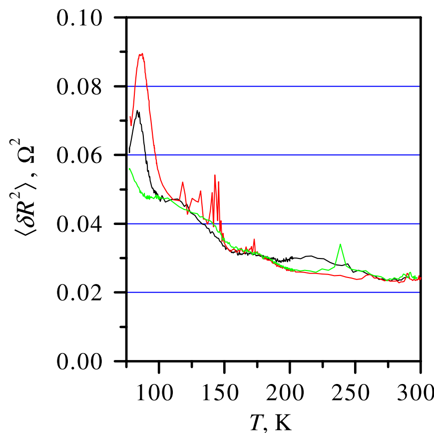

Figure 6. Noise power (resistance fluctuations) in the band 10–100 Hz versus temperature measured three times (every two days) on terminations 1–7 of the R344/P304PtAu resistor under the bias $I \cong 69\,\mu$A.

as the maximum spread of noise power values measured in successive temperature cycles. In figure 4(*b*) this occurs at ~150 K where noise powers differ by more than a factor of 2. Larger spreads of the values were observed in long-time experiments. For v12RuO$_2$/P303Au samples the measurements were performed several times for four months. Results collected in figure 5(*a*) show that at certain temperatures noise power can change even by an order of magnitude. In figure 6 similar data for a R344/P304PtAu resistor are shown. This resistor is made of conductive and resistive pastes that are both from the same manufacturer (ITME). They (i.e. the pastes) were designed to form a compatible 'system' for high-quality resistors. Despite this, TANSs and N/M fluctuations are observed below 110 K: these phenomena are not just the feature of our lab-made compositions but rather a common property of TFRs, which considerably diminishes their performance.

In the measurements reported in figures 4(*b*), 5(*a*), and 6 different noise spectra were observed in certain temperature ranges in several cooldowns of the sample. An important question is how the spectra changed their shape—was it an abrupt switching-like event or continuous evolution? The answer comes from another noise power versus temperature measurement. A set of noise maps in figure 7 demonstrates that spectra do not continuously evolve but rather switch from one shape to another. Data in figure 7 were recorded for v10RuO$_2$/P303Au resistors in successive temperature cycles. Maps (*a*)–(*d*) were measured on terminations 1–7. In (*a*) and (*b*), with increasing temperature, the system switches from 'noise state I' characterized by TANS of activation energy $E_a \cong 0.34$ eV to 'noise state II' characterized by TANS of activation energy $E_a \cong 0.37$ eV. In (*c*) the system stays in state II. In (*d*) it stays in state I. In those two states noise spectra, e.g. at ~200 K have different shapes. From time-thermal history we know that the change in the spectrum shape was by abrupt switching.

Maps (*e*) and (*f*) in figure 7 refer to terminations 1–2 and 2–6, respectively. Map (*e*) was measured simultaneously with map (*a*) whereas (*f*) simultaneously with (*b*). In (*a*) and (*b*) the switching was detected. No traces of the switching are observed in (*e*) unlike in map (*f*) where the switching is clearly visible. This means that the source of the switching event lies somewhere in sectors 2–6 or, according to the discussion in section 5.3, slightly above/below contact 6/2. This conclusion violates our earlier opinion that N/M fluctuations may occur only in the interface area.

Data in figure 8 illustrate that the switching process can take a course of several attempts. TANS which in figure 8(*b*) gives a clear contrast in low temperatures switches off in a four-step process in which the system recovers the final state with the pure $1/f$ spectrum through intermediate 'noise states'. This was observed for DP2031/Fodel microresistors and additionally documents that switching between various noise spectra is also a commonly observed phenomenon.

6.1. Short pulses

N/M fluctuations leading to an abrupt change in noise spectra while changing the temperature often take the form of short pulses. These pulses mostly appear in groups of several events but individual switchings have also been observed. Examples of pulse switching (PS) processes might have been observed in figures 3, 5 and 6.

In figure 3(*a*) PS appears in the experiment on contacts 3–5 of the R344/1130CPtAg resistor. It switches the *whole*

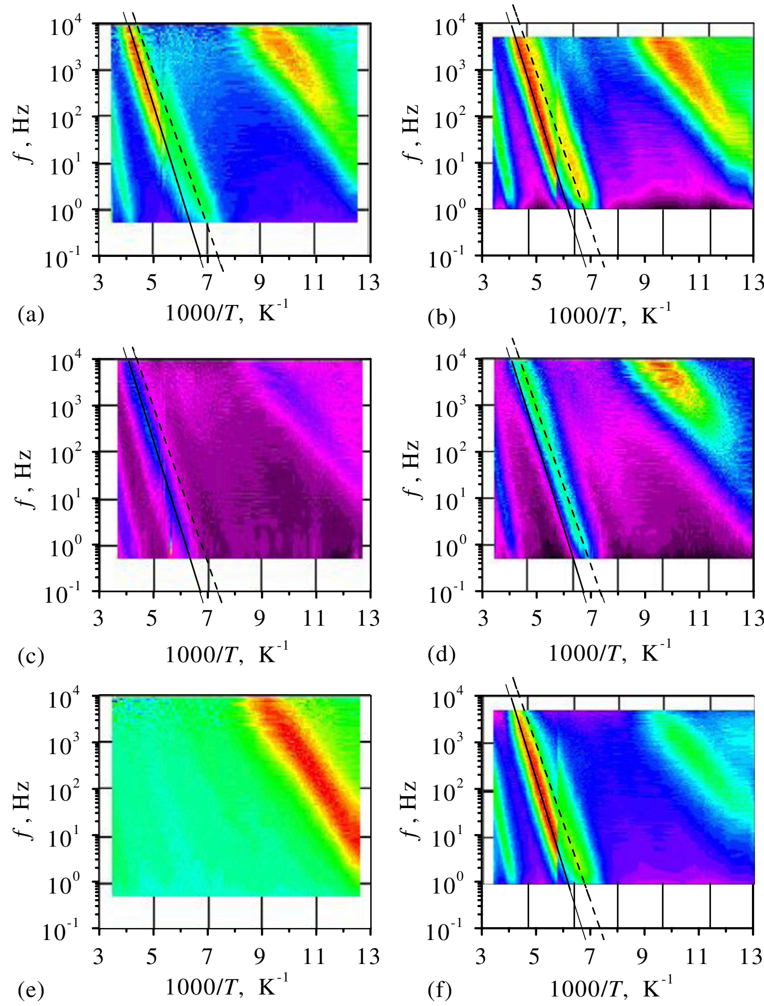

Figure 7. (*a*)–(*d*) Maps of the product $f\,S_V(f)/V^2$ recorded on contacts 1–7 of v10RuO$_2$/P303Au resistors. In all the maps lines are the plots of $f_{\rm max} = f_0 \exp(-E_{\rm a}/kT)$ with $E_{\rm a} = 0.37$ eV (——) or 0.34 eV (- - - -). (*e*) and (*f*) Maps recorded on contacts 1–2/2–6 simultaneously with maps (*a*) and (*b*).

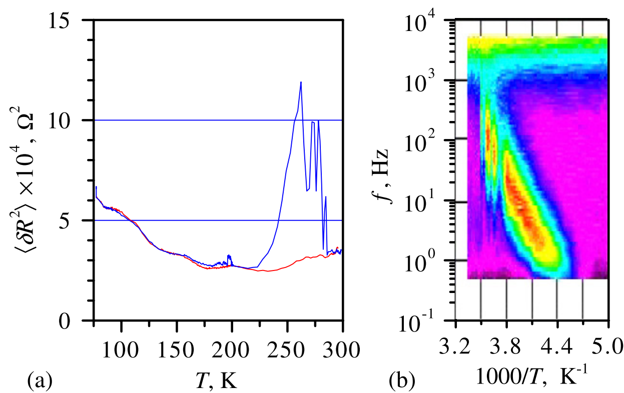

Figure 8. (*a*) Noise power (resistance fluctuations) in the band 10–100 Hz versus temperature measured twice on terminations 1–7 of the DP2031/Fodel resistor under the bias $I \cong 0.21$ mA. (*b*) Map of the product $f\,S_R(f, T)$ recorded during one of the measurements.

3–5 spectrum to values higher by some 25%, so that the vertical streak in map '3–5' (figure 3(*b*)) extends along the whole frequency axis. The process is also observed on terminations 1–7 but its physical source is localized inside the resistor (in sector 3–5 or very close to it).

Figure 5(*b*) contains the noise map measured for the v12/P303Au resistor in one of several thermal cycles (see (*a*) in this figure). PS took place near $T = 197$ K ($1000/T \cong 5.08$ K^{-1}) and changed only the magnitude of TANS that produced the main streak in the map, leaving the rest of the spectrum unchanged. The TANS magnitude was suppressed by a factor of $\sim$3 as can be estimated from figure 5(*c*) where noise spectra (scaled by the actual frequency to compress $1/f$ dynamics) measured at temperatures marked in map (*b*) as A (198 K), B (197 K) and C (196 K) are shown. At higher frequencies spectra are dominated by thermal noise and remain unchanged while the system switches between different spectra. This observation is of some importance as it ensures that PS at 197 K (i) has not been recorded because of temporary malfunction of the measurement setup and (ii) affects only the excess noise.

In figure 5(*a*) the switching process on the curve labelled '90' produces a pulse of negative value. A burst of pulses but of positive values was observed in the experiment on R344/P304PtAu resistors (figure 6) made from the manufacturer-optimized system of pastes. Further examples include resistors with Ag-containing termination and resistors

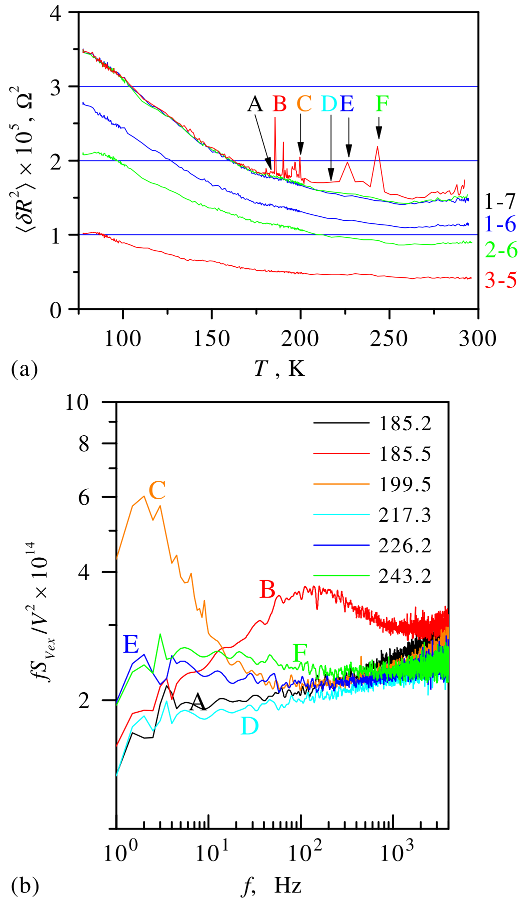

Figure 9. (*a*) Noise power (resistance fluctuations) in the band 10–100 Hz versus the temperature measured on various contacts of the R343/1130CPtAg resistor subjected to the bias $I \cong 0.41$ mA. Labels on the right of the figure specify sectors for which noise power has been measured. Labels A–F inside the figure specify temperatures for which noise spectra are shown in (*b*).

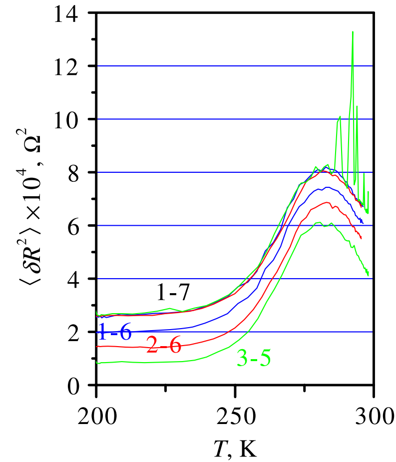

Figure 10. Noise power (resistance fluctuations) in the band 10–100 Hz versus temperature measured on various contacts of v12RuO$_2$/3612Au resistors fired at 900 °C subjected to the bias $I \cong 0.17$ mA. Labels on the left side of the plots specify contacts from where the noise signal had been acquired.

fabricated in various technological processes. In figure 9(*a*) plots of noise power versus temperature recorded in three day-by-day coolings of R343/1130CPtAg resistors are shown. For these low-ohm resistors the noise power decreases with increasing temperature but no TANS has been found in the temperature range 77–300 K. In one experiment a series of PS was observed on terminations 1–7 when the temperature passed from 185 to 245 K. Noise spectra measured at selected temperatures, labelled A–F, are shown in figure 9(*b*). As one can see at temperatures A, D and E, F spectra are flat and differ merely in magnitude. At temperatures B and C the system (unsuccessfully) attempts to turn TANSs of different activation energies.

Figure 10 demonstrates that the PS process survives the change in the important parameters of the resistors' fabrication process. Data were collected for the v12RuO$_2$/3612Au resistor which was fired at 900 °C. The maximum in the noise power versus temperature observed at ~280 K is produced by TANS of $E_a = 0.57$ eV. PS was observed during one of the temperature cycles when noise spectra were acquired simultaneously on contacts 3–5 and 1–7. Switching was observed on contacts 1–7 but the spectra taken for the inner part of the resistor were not affected by this process. With this regard they are similar to the previous examples of the PS process. In all but one cases PS was observed on the terminations that include at least one conductive/resistive film interface. The only exception was the R344/1130CPtAg resistors (see figure 3) for which PS was observed also for the inner part of the resistor. The set of examples was not selected tendentiously and reflects the actual relation observed in the measurements. We are entitled to conclude that, although not exclusively, the PS process should be attributed to the regions where resistive and conductive films form an interface. This statement is not valid for LTCC resistors as is discussed later.

6.2. *Switching phenomena*

Switching phenomena discussed above affect the excess noise which has been identified as resistance fluctuations. For inhomogeneous systems such as TFRs the fluctuations of the resistance δR are the weighting sum of local resistance fluctuations, with weighting coefficients being just the ratio of the local current I_k to the total current I (see (4)). δR is especially sensitive to those fluctuators k that carry large local currents I_k. Any change (redistribution) in these currents makes the fluctuation δR sensitive to another set of local fluctuators and in the case of their inhomogeneous distribution leads to the change in the noise spectrum. Reasons for current redistribution can be different.

6.3. *Dynamic current redistribution*

One possibility is dynamic redistribution triggered by the noise itself [24–26]. In this scenario a fluctuator in one of its states not only changes the magnitude of local resistance but can also block or open a new conducting channel and redistribute local currents. Dynamic current redistribution (DCR) has been confirmed to produce nonGaussian fluctuations in a large volume carbon-composite resistor [27]. This mechanism is of purely statistical nature and is expected to be observed both in

long-time experiments at constant temperature and in thermal cycling.

The fluctuators that can switch the system between different current patterns have different (widely scattered) rates. Those with rates much faster than the time scale of the experiment contribute to the noise spectrum at higher frequencies. Those with rates comparable to the time scale of the experiment can be observed in the time domain as *reproducible* switchings between (two) different noise spectra. These spectra are built up by the fluctuators that become active while DCR takes place. The most probable candidates for fluctuators that are able to redistribute local currents are TANSs. The statistics of switching events (e.g. the average time the system stays in one state) should then obey the thermally activated (Arrhenius) law. This condition is certainly not fulfilled by the PS process that often occurs in bursts of several pulses separated by long PS-free periods. In contrast, the process that switches the system between two noise states in figure 7 is a good candidate to be caused by DCR.

6.4. Stress relaxation

Another possibility is that the current redistributes in response to the relaxation of mechanical stress which in TFR appears due to the mismatch of thermal expansion coefficients of the composite materials and the ceramic substrate. The production process implies that *internal* stress appears in TFR only when it cools down after the firing. This stress relaxes then slowly, as defects are created or removed, and/or micro-cracks develop in the overglaze formed on the TFR. These relaxation processes occurred to be basic sources of resistance drift observed in many experiments [7, 16, 28, 29]. In stress relaxation temperature plays an important role. It was shown that ageing resistors at 100–200 °C can significantly accelerate relaxation phenomena [7, 30]. Thermal cycling applied to the resistors in our study is quite different from that used while ageing. The samples were cooled, instead of heated, which slows down the relaxation phenomena. On the other hand changing the temperature by a factor of ∼4 results in extra stress which adds up to the internal stress in every cooling–warming cycle. Resistors respond to the *total* stress. Thus, the events through which relaxation takes place mirror the whole time-thermal history of the sample and are not reproducible in successive coolings. Even more important in this issue is that the spatial distribution of local stress changes after each relaxation event. In this way one event influences future events: the relaxing stress at some point may result in stress increase at some other point and enhanced probability of relaxation at this point. Thus, stress relaxation is likely to occur in sequences of several steps. As stress redistributes locally the relaxation events that come in bursts are capable of controlling the same branch of the percolation cluster. It is then possible that different mechanical events result in a similar electrical response. For example, the developing group of several cracks may block or open a percolation path giving rise to observable switching between merely two or three electrical (noise) states. Note eventually that the burst of events observed as burst of switchings is certainly not thermally activated in the sense of equation (1) (f_{max} corresponds to the average switching period). All the features, mentioned above, could be recognized in figures 3, 5, 6, 8–10 suggesting that the PS process described in section 6.1 is likely to be triggered by stress relaxation. Probably most of the microstructural fluctuations occurring during temperature cycles also result from stress relaxation.

Independently of the physical origin the spatial extent of current redistribution can be much larger than the homogenization length. In the worst case a fluctuator can block the critical bond (resistance) of the percolation path. Then the redistribution of currents extends over the volume of many percolation correlation lengths. The latter for TFRs does not exceed several tens of micrometres; so the phenomenon can still be considered as local property that could redistribute currents in one sector of the resistor leaving the currents in other sectors unchanged. In the DCR mechanism noise sources are distributed throughout the whole resistor and DCR induced switchings are likely to occur in the whole resistor volume. In contrast, stress localizes in film/substrate and conductive/resistive film interfaces where the number of various ingredients is the largest. Switchings triggered by stress relaxation are preferred to occur in resistor interfaces.

6.5. Interacting fluctuators

Yet another possibility is that current does not redistribute but fluctuators change their magnitude. It is possible when they interact with each other. In this picture the amplitude of the fast fluctuator depends on the actual state of some slow fluctuators. When the latter changes its state the noise spectrum changes its magnitude at the frequency of the fast fluctuators. To some extent this mechanism is similar to DCR where interactions between fluctuators are transferred by the flowing current. Interacting fluctuators have been found in glassy materials [31], so it is possible to find them also in TFRs which contain large amount of glasses.

7. Discussion and summary

The use of low frequency noise spectroscopy revealed interesting properties of resistive film film/substrate and film/termination interfaces of TFR. These are TANSs and switching phenomena. Features that characterize TANSs are listed in the beginning of section 5. Most of them have been discussed in detail. Those not explicitly commented can be inferred from numerous figures illustrating noise and switching phenomena occurring in the films. Figure 9 demonstrates, e.g. that low-resistive films (R343—1 kΩ/□) have much smaller (if any) number of TANSs than resistors of a higher sheet resistance. Probably, this is a more general property which also makes resistors fired at lower temperatures to have less intensive TANSs than those fired at higher temperatures. Experiments made on the v12RuO_2 series show that resistors fired at lower temperatures always have lower sheet resistances. A pair of plots in figure 11 made for v12RuO_2/P304PtAu resistors fired at 800 and 900 °C show that, indeed, the noise signal generated by TANSs is less intensive for resistors fired at a lower temperature.

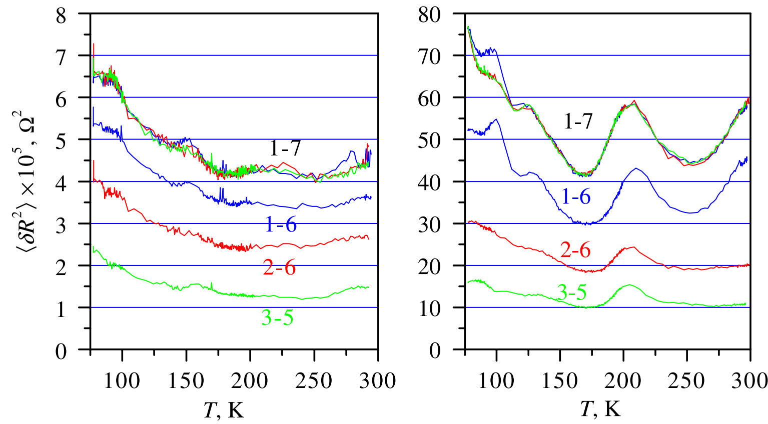

Figure 11. Noise power (resistance fluctuations) in the band 10–100 Hz versus temperature measured on various contacts of v12/P304Au resistors fired at peak temperature $T_f = 800\,^\circ$C (left) or 900 °C (right).

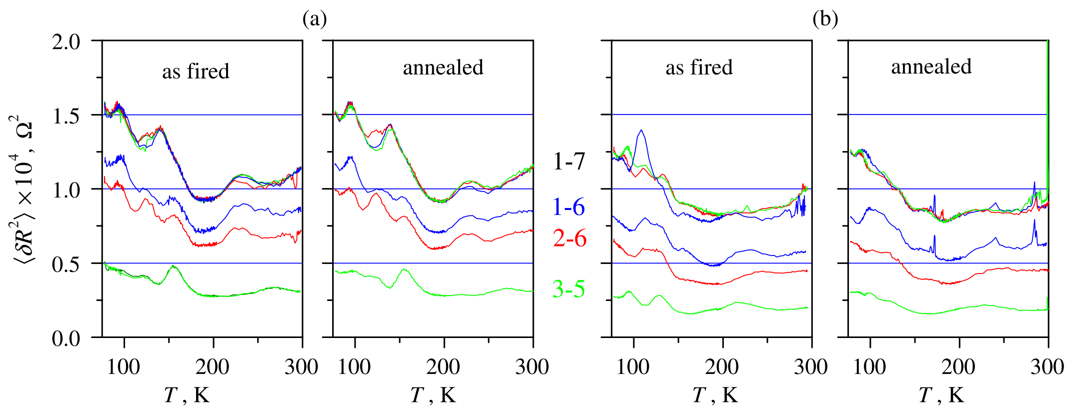

Figure 12. Noise power (resistance fluctuations) in the band 10–100 Hz versus temperature measured on various contacts of (*a*) v12RuO$_2$/3612Au and (*b*) v12RuO$_2$/P304Au resistors before and after annealing.

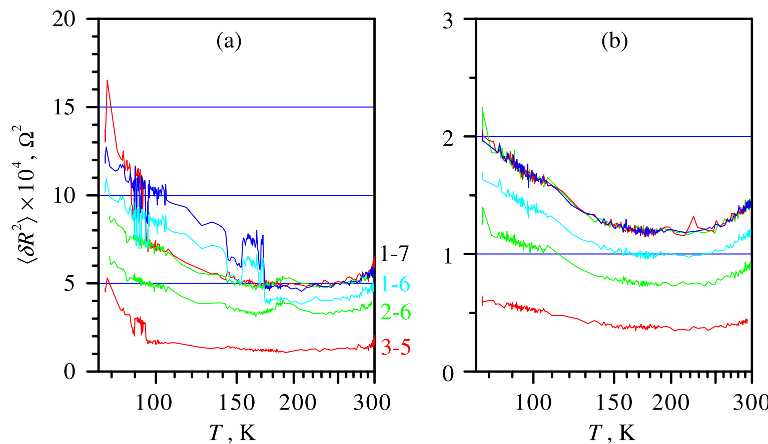

Figure 13. Noise power (resistance fluctuations) in the band 1–10 Hz versus temperature measured on various contacts of LTCC DP2041/DP6146PdAg resistors fabricated in (*a*) post-fired and (*b*) co-fired processes.

The next pairs of plots in figure 12 demonstrate that localization of TANSs and their magnitudes do not change significantly (that is more than that due to N/M processes) after annealing. Eventually, figure 13 shows several noise power versus temperature plots collected for LTCC resistors. These plots are slightly different from those for the resistors on alumina substrates. A maximum on the $\langle \delta R^2_{3-5} \rangle (T)$ plot for post-fired DP2041/DP6146PdAg resistors moves with temperature and can be attributed to TANS. Two-level switching observed on the $\langle \delta R^2_{1-6} \rangle (T)$ and $\langle \delta R^2_{1-7} \rangle (T)$ plots is due to N/M fluctuation but in this case we rather attribute it to the relaxation of the stress that localizes on the film/substrate interface. Resistive films of post-fired resistors were fired on previously fired LTCC substrates and are not so well attached to them as the resistors made in a co-fired process. Indeed, data in figure 13 collected for the DP2041/DP6146PdAg resistor

made in the co-fired process show no switching events at all. A similar relation has been observed for DP2041/ESL8880HAu resistors with gold contacts.

Summing up, experiments reported in the paper show that the common property of TFRs are TANSs that localize in glass or conductive grain boundaries and are nonuniformly distributed in the whole resistor volume, in many cases more frequently in the resistive/conductive films interface. These noise sources are subjected to switching phenomena which abruptly change the shape and magnitude of the noise spectrum. The physical origin of the switching process is less clear. Although most likely it is a redistribution of local currents driven by the relaxation of mechanical stress, further studies are needed to draw definite conclusions.

Both phenomena are very common and take place even in manufacturer-optimized systems of compatible pastes and substrates. Of large practical implication is that switching and/or nonstationary TANSs occur in the temperature range covered by the standard operation of TFRs. Moreover, both phenomena become more intensive well below room temperature in the very demanding area of applications in aviation industry, space exploration and astrophysics. What makes things even worse is that both phenomena are known to be connected with device stability and reliability. Similar objections may be raised when thinking about cryogenic application. Here, noise and switching phenomena could spoil the application of chip TFRs as low-temperature sensors [32] and bolometers.

Acknowledgments

The work was supported by the Polish Ministry of Science and Higher Education through grant No 3T11B 070 29. Fruitful discussions with R Śliwa on stress and fracture in layered composite material are also gratefully acknowledged.

References

[1] Vandamme L K J 1977 *Electrocompon. Sci. Technol.* **4** 171
[2] Vandamme L K J 1994 *IEEE Trans. Electron. Devices* **41** 2176
[3] Roesner B and Witte W 1989 *Proc. 1989 Int. Symp. on Microelectronics (Baltimore, MD, 1989)* ed H K Charles Jr *et al* (Reston, VA: Int. Soc. Hybrid Microelectron.) p 175
[4] Dutta P, Dimon P and Horn P M 1979 *Phys. Rev. Lett.* **43** 646
[5] Skrbek L, Stehno J and Sebek J 1996 *J. Low Temp. Phys.* **103** 209
[6] Jones B K 1994 *IEEE Trans. Electron Devices* **41** 2188
[7] Coleman M 1984 *Hybrid Circuits* **4** p 36
[8] Dziedzic A 1989 *Microelectron. J.* **19** 24
[9] Yamaguchi T and Kageyama M 1988 *IEEE Trans. Compon. Hybrids Manuf. Technol.* **11** 134
[10] Pellegrini B, Saletti R, Terreni P and Prudenziati M 1983 *Phys. Rev.* B **27** 1233
[11] Chen T M, Su S F and Smith D 1982 *Solid State Electron.* **25** 821
[12] Masoero A M, Rietto B, Morten and Prudenziati M 1983 *J. Phys. D: Appl. Phys.* **16** 669
[13] Jakubowska M 2007 private communication
[14] See, e.g. Abe O and Taketa Y 1991 *J. Phys. D: Appl. Phys.* **24** 1163
[15] Dziedzic A, Rebenklau L, Golonka L J and Wolter K-J 2003 *Microelectron. Reliab.* **43** 377
[16] Murthy K S R C and Kumar V A 1990 *J. Mater Sci. Mater. Electron* **1** 61
[17] Khanna P K, Bhatnagar S K and Gust W 1994 *Phys. Status Solidi* a **143** K33
[18] Kolek A, Ptak P, Mleczko K and Wrona A 2001 *Proc. 16th Int. Conf. on Noise in Physical Systems and 1/f Fluctuations (Gainesville, FL, 2001)* ed G Bosman (Singapore: World Scientific) p 713
[19] Clarke J and Voss R F 1974 *Phys. Rev. Lett.* **33** 24
[20] Zeller R C and Pohl R O 1971 *Phys. Rev.* B **4** 2029
[21] For a review of $1/f$ noise phenomenon see, e.g. Hooge F N, Kleinpenning T G M and Vandamme L K J 1981 *Rep. Prog. Phys.* **44** 479
[22] Kolek A, Stadler A W, Zawislak Z and Mleczko K 2007 *Proc. 19th Int. Conf. Noise and Fluctuations (Tokyo, 2007)* vol 922, ed M Tacano *et al* (Melville, NY: AIP Conf. Proc.) p 273
[23] Vandamme L K J and van Bokhoven W M G 1977 *Appl. Phys.* **14** 205
[24] Lust L M and Kakalios J 1995 *Phys. Rev. Lett.* **75** 2192
[25] Abkemeier K M and Grier D G 1996 *Phys. Rev.* B **54** 2723
[26] Seidler G T, Solin S A and Marley A C 1996 *Phys. Rev. Lett.* **76** 3049
[27] Seidler G T and Solin S A 1996 *Phys. Rev.* B **53** 9753
[28] Smith B L 1989 *Packaging Electronic Materials Handbook* vol 1, ed M L Minges (Materials Park, OH: ASM International) p 994
[29] Shah J S 1980 *IEEE Trans. Compon. Hybrids Manuf. Technol.* **3** 554
[30] De Schepper L, De Ceuninck W, Stulens H, Stals L M, Vanden Berghe R and Demolder S 1990 *Hybrid Circuits* **23** 5
[31] Weissman M B 1993 *Rev. Mod. Phys.* **65** 829
[32] Ptak P, Kolek A, Zawiślak Z, Stadler A W and Mleczko K 2005 *Rev. Sci. Instrum.* **76** 014901